Journal of the Physical Society of Japan
Vol. 73, No. 7, July, 2004, pp. 1922–1930

Josephson Effect in Quasi One-dimensional Unconventional Superconductors

Yasuhiro ASANO, Yukio TANAKA[1,2], Yasunari TANUMA[3], Kazuhiko KUROKI[4] and Hiroki TSUCHIURA[5]

Department of Applied Physics, Hokkaido University, Sapporo 060-8628
[1]*Department of Applied Physics, Nagoya University, Nagoya 464-8603*
[2]*Crest, Japan Science and Technology Corporation (JST), Nagoya 464-8063*
[3]*Institute of Physics, Kanagawa University, Yokohama 221-8686*
[4]*Department of Applied Physics and Chemistry, The University of Electro-Communications, Chofu, Tokyo 182-8568*
[5]*SISSA, via Beirut 2-4, 34014 Trieste, Italy*

(Received October 13, 2003)

Josephson effect in junctions of quasi one-dimensional superconductors at the quarter-filling electron density is discussed by using the tight-binding model on a two-dimensional square lattice. To consider the triangular lattice structures in real materials such as $(TMTSF)_2X$ ($X = PF_6$, ClO_4, etc), the asymmetric hopping integral is introduced among second nearest lattice sites. A combination of these characters in superconductors (quasi one-dimensionality, quarter-filling electron density and weak triangular lattice structures) seriously affects the formation of a zero-energy state at a junction interface. As a consequence, calculated results of the Josephson current show anomalous dependences on temperatures.

KEYWORDS: organic superconductor, zero-energy states, low-temperature anomaly, quarter-filling, quasi one-dimension
DOI: 10.1143/JPSJ.73.1922

1. Introduction

The Josephson effect is a result of the Andreev reflection[1)] of a quasiparticle incident into a superconductor from a normal metal.[2)] In unconventional superconductors, the pair potential of an incident quasiparticle in the electron branch is different from that in the hole branch. When the two pair potentials have opposite signs, a constructive interference of a quasiparticle causes the formation of a zero-energy state (ZES) at a surface of a superconductor.[3–9)] The ZES drastically affects transport properties through the surfaces of superconductors because it appears just on the Fermi energy. For instance, a large peak at the zero bias voltage in tunneling spectra of unconventional superconductors is a direct consequence of the ZES.[5,10–16)] The low-temperature anomaly of the Josephson current between the two unconventional superconductors is explained in terms of the resonant tunneling of Cooper pairs through the ZES.[17–28)] In theories, so far, the Andreev reflection has been studied by using the free electron model in which the quadratic dispersion relation and the isotropic Fermi surface are assumed. Although the Fermi surfaces in real superconductors are not isotropic *at al.*, calculated results based on the free electron model well explain experimental results. This fact implies that the Andreev reflection might be insensitive to electronic structures in superconductors and that it would be sensitive only to pairing symmetries. However, recent theoretical studies showed several exceptions.[26,29)] The density of states at the surface of organic superconductors $(TMTSF)_2X$ ($X = PF_6$, ClO_4, etc.)[30,31)] depends strongly on the shape of the quasi one-dimensional (Q1D) Fermi surface when triangular lattice structures are taken into account in the superconductor.[29,32)]

In $(TMTSF)_2X$, unconventional superconductivity has suggested from a number of experiments such as large H_{c2},[33)] unchanged Knight shift across T_c,[34)] an NMR measurement,[35)] a thermal conductivity measurement[36)] and the zero-bias conductance peak (ZBCP) in tunnel spectra.[37)] Theoretically, a p wave paring has been proposed in an early stage.[38–40)] On the other hand, a spin-singlet d wave pairing mediated by spin fluctuations has been proposed by several authors.[41–43)] Moreover, one of authors has recently proposed that[44)] a triplet f wave pairing may dominate over the d and the p wave in $(TMTSF)_2PF_6$. A combination of a Q1D Fermi surface, coexistence of the $2k_F$ spin density wave and the $2k_F$ charge density wave,[45,46)] and an anisotropy in the spin fluctuations enables the f wave symmetry.

Motivated by results of the surface density of states in Q1D superconductors,[29,32,47)] we will discuss the direct-current Josephson effect between two organic superconductors. The purpose of this paper is to make clear effects of the quasi one-dimensionality, those of the quarter-filling electron density and those of the triangular lattice structures on the Josephson current. So far, a theoretical paper[48)] has reported the Josephson effect in organic superconductors. However these issues were not discussed. For the purpose, we describe the organic superconductors by using the tight-binding model on a two-dimensional square lattice. The quasi one-dimensionality is taken into account through the anisotropy of the hopping integrals in the two directions. To consider the triangular lattice structures in real materials, we also introduce the asymmetric hopping integral among second nearest lattice sites. In superconductors, we assume pair potentials with p, d and f wave like pairing symmetries. The Josephson current is numerically calculated by using the lattice Green function method.[49–51)] A combination of the quasi one-dimensionality, the quarter-filling electron density and the weak triangular lattice structures seriously affects the formation of a zero-energy state at a junction interface. As a consequence, calculated results of the Josephson current show anomalous dependences on temperatures.

This paper is organized as follows. In §2, we described the Josephson junctions of organic superconductors by the Bogoliubov–de Gennes equation on the two-dimensional lattice. The Josephson current is discussed for p, d and f

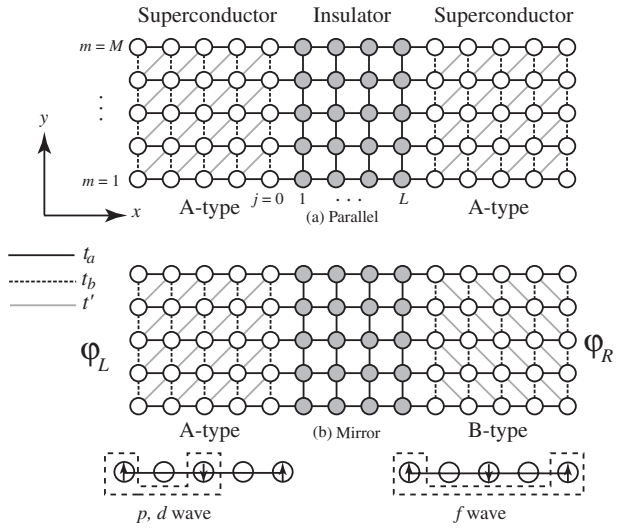

Fig. 1. A schematic figure of the SIS junction of the organic superconductor.

wave symmetries in §3. In §4, we discuss the calculated results. We summarize this paper in §5.

2. Model and Method

Let us consider Q1D superconductor/insulator/superconductor (SIS) junctions as shown in Fig. 1. A vector $\boldsymbol{r} = j\bar{\boldsymbol{x}} + m\bar{\boldsymbol{y}}$ points a lattic site, where $\bar{\boldsymbol{x}}$ and $\bar{\boldsymbol{y}}$ are the unit vectors in the x and the y directions, respectively. The two superconductors (i.e., $-\infty \le j \le 0$ and $L+1 \le j \le \infty$) are separated by the insulator (i.e., $1 \le j \le L$). We assume the periodic boundary condition in the y direction. The number of lattice sites in the y direction is M. The superconducting junctions are described by the mean-field Hamiltonian

$$H_{\rm BCS} = \frac{1}{2}\sum_{\boldsymbol{r},\boldsymbol{r}'}\left[\tilde{c}_{\boldsymbol{r}}^{\dagger} h_{\boldsymbol{r},\boldsymbol{r}'}\hat{\sigma}_0\tilde{c}_{\boldsymbol{r}'} - \tilde{c}_{\boldsymbol{r}}^{t} h_{\boldsymbol{r},\boldsymbol{r}'}^{*}\hat{\sigma}_0\left\{\tilde{c}_{\boldsymbol{r}'}^{\dagger}\right\}^{t}\right] + \frac{1}{2}\sum_{\boldsymbol{r},\boldsymbol{r}'\in {\rm S}}\left[\tilde{c}_{\boldsymbol{r}}^{\dagger}\hat{\Delta}_{\boldsymbol{r},\boldsymbol{r}'}\left\{\tilde{c}_{\boldsymbol{r}'}^{\dagger}\right\}^{t} - \{\tilde{c}_{\boldsymbol{r}}\}^{t}\hat{\Delta}_{\boldsymbol{r},\boldsymbol{r}'}^{*}\tilde{c}_{\boldsymbol{r}'}\right], \quad (1)$$

$$h_{\boldsymbol{r},\boldsymbol{r}'} = -t_{\boldsymbol{r},\boldsymbol{r}'} + (\epsilon_{\boldsymbol{r}} - \mu_{\boldsymbol{r}})\delta_{\boldsymbol{r},\boldsymbol{r}'}, \quad (2)$$

$$\hat{\Delta}_{\boldsymbol{r},\boldsymbol{r}'} = \begin{cases} {\rm i}\boldsymbol{d}_{\boldsymbol{r},\boldsymbol{r}'}\cdot\hat{\boldsymbol{\sigma}}\hat{\sigma}_2 \text{: triplet} \\ {\rm i}d_{\boldsymbol{r},\boldsymbol{r}'}\hat{\sigma}_2 \quad \text{: singlet,} \end{cases} \quad (3)$$

$$\tilde{c}_{\boldsymbol{r}} = \begin{pmatrix} c_{\boldsymbol{r},\uparrow} \\ c_{\boldsymbol{r},\downarrow} \end{pmatrix}, \quad (4)$$

where $c_{\boldsymbol{r},\sigma}^{\dagger}$ ($c_{\boldsymbol{r},\sigma}$) is the creation (annihilation) operator of an electron at $\boldsymbol{r}$ with spin $\sigma = (\uparrow$ or $\downarrow)$, $\hat{\sigma}_0$ is the 2×2 unit matrix representing the spin space, $\hat{\sigma}_j$ with $j = 1$–3 are the Pauli matrices and S in the summation denotes the superconductors. The Fermi energy in the superconductor is $\mu_{\boldsymbol{r}} = \mu_{\rm S}$ for $j \le 0$ and $j \ge L+1$, and that in the insulator is $\mu_{\boldsymbol{r}} = \mu_{\rm N}$ for $1 \le j \le L$. In superconductors, $\epsilon_{\boldsymbol{r}}$ is taken to be zero, and t_a and t_b are the hopping integral in the x and the y directions, respectively. We also introduce the asymmetric hopping integral (t') between the second nearest neighbors as shown in Fig. 1 to realize electronic structures in $(TMTSF)_2PF_6$. In the insulator, $\epsilon_{\boldsymbol{r}} = V_{\rm B}$ for $1 \le j \le L$ represents the barrier potential and the hopping integrals in the two directions are equal to t_a. The pair potential in p, d and f wave symmetries are defined by,

$$\boldsymbol{d}_{\boldsymbol{r},\boldsymbol{r}'}^{(p)} = \frac{\Delta}{2}{\rm sgn}(j-j')\delta_{|j-j'|,2}\delta_{m,m'}\boldsymbol{e}_3, \quad (5)$$

$$d_{\boldsymbol{r},\boldsymbol{r}'}^{(d)} = \frac{\Delta}{2}\delta_{|j-j'|,2}\delta_{m,m'}, \quad (6)$$

$$\boldsymbol{d}_{\boldsymbol{r},\boldsymbol{r}'}^{(f)} = \frac{\Delta}{2}{\rm sgn}(j-j')\delta_{|j-j'|,4}\delta_{m,m'}\boldsymbol{e}_2, \quad (7)$$

where $\boldsymbol{e}_j$ with $j = 1$, 2 and 3 are unit vectors in the spin space. The macroscopic phase factor $e^{i\varphi_L}$ or $e^{i\varphi_R}$ should be mutiplied to the pair potentials when we calculate the Josephson current. A schematic picture of Cooper pairs is shown in Fig. 1. The pair potential in eqs. (5), (6) and (7) are proposed in theoretical papers. At the quarter filling electron density, it is reasonable to consider the pairing correlation between two electrons localized at the second nearest neighbor sites as shown in Fig. 1. The spins of the neighboring electrons tend to align opposite direction. As a consequence, the two neighboring spins form a singlet pair or a triplet one. A Quantum Monte Carlo study[42] on the Hubbard model showed that spin correlation function has a peak at a nesting vector $(k_a, k_b) = (\pi/2, \pi)$, where k_a and k_b are the wavenumber in the x and the y direction, respectively. Such spin structure favors a superconducting order parameter in eq. (6). The possibility of the order parameter in eq. (6) was also pointed out in a diagrammatic expansion.[41] Equation (6) is a natural solution when the two neighboring spins form a spin-singlet pair. On the other hand, a possibility of the spin-triplet pairing was pointed out in several papers.[38–40,44] The spin-triplet symmetry requires the anti-symmetric pair potential in the momentum space, which causes the node line at $k_a = 0$. The condensation energy, however, is well preserved because the node line does not intersect the Q1D Fermi surface.[39] Equation (5) is a natural solution when the two neighboring spins form a spin-triplet pair with $S_y = 0$ in the presence of an anisotropy in the spin–spin correlation.[52] Actually the easy axis of spins is the b axis parallel to the y direction. One of authors also proposed eq. (7) based on results of the fluctuation-exchange calculation.[44] The coexistence of the $2k_{\rm F}$ spin and charge fluctuations favors the pairing correlation between two electrons at fourth nearest neighbor sites in the presence of an anisotropy in the spin–spin correlation. These pair potential may remain qualitatively unchanged even in the presence of $|t'| \ll t$ because the spin and the charge fluctuations along the chain direction, the quasi one-dimensionality and the anisotropy of the spin–spin correlation are important ingredients in the argument above.[44] Thus eqs. (5)–(7) are highly possible candidates of pair potentials in Q1D superconductors at the quarter-filling electron density such as $(TMTSF)_2X$.

The two spin-triplet pair potentials in eqs. (5) and (7) are basically belonging to the same symmetry class. Thus they are possible to coexist. Especially this may happen at the junction interface because the interface might suppress the coexistence of the $2k_{\rm F}$ spin and the charge fluctuations which favors eq. (7). As well as a paring symmetry in bulk, a symmetry at a surface or a hetero structure interface is very important issue to understand nature of superconductivity.[53] At present, however, we have only limited information on this issue. In this paper, at the first step of studying the quantum transport in organic superconductors, we distin-

guish eq. (5) from (7) because the purpose of this paper is to study effects of the quasi-one dimensionality, the quarter-filling electron density and triangular lattice structures on the Josephson current.

The Hamiltonian is diagonalized by the Bogoliubov transformation,

$$\begin{bmatrix} \tilde{c}_{\boldsymbol{r}} \\ \{\tilde{c}^{\dagger}_{\boldsymbol{r}}\}^t \end{bmatrix} = \sum_{\lambda} \begin{bmatrix} \hat{\boldsymbol{u}}_{\lambda}(\boldsymbol{r}) & \hat{\boldsymbol{v}}^{*}_{\lambda}(\boldsymbol{r}) \\ \hat{\boldsymbol{v}}_{\lambda}(\boldsymbol{r}) & \hat{\boldsymbol{u}}^{*}_{\lambda}(\boldsymbol{r}) \end{bmatrix} \begin{bmatrix} \tilde{\gamma}_{\lambda} \\ \{\tilde{\gamma}^{\dagger}_{\lambda}\}^t \end{bmatrix}, \tag{8}$$

$$\tilde{\gamma}_{\lambda} = \begin{pmatrix} \gamma_{\lambda,\uparrow} \\ \gamma_{\lambda,\downarrow} \end{pmatrix}, \tag{9}$$

where $\gamma^{\dagger}_{\lambda,\sigma}$ ($\gamma_{\lambda,\sigma}$) is the creation (annihilation) operator of a Bogoliubov quasiparticle. In eq. (8), $\hat{\boldsymbol{u}}_{\lambda}$ and $\hat{\boldsymbol{v}}_{\lambda}$ satisfy the Bogoliubov–de Gennes (BdG) equation,[54]

$$\sum_{\boldsymbol{r}'} \begin{bmatrix} h_{\boldsymbol{r},\boldsymbol{r}'}\hat{\sigma}_0 & \hat{\Delta}_{\boldsymbol{r},\boldsymbol{r}'} \\ -\hat{\Delta}^{*}_{\boldsymbol{r},\boldsymbol{r}'} & -h^{*}_{\boldsymbol{r},\boldsymbol{r}'}\hat{\sigma}_0 \end{bmatrix} \begin{bmatrix} \hat{\boldsymbol{u}}_{\lambda}(\boldsymbol{r}') \\ \hat{\boldsymbol{v}}_{\lambda}(\boldsymbol{r}') \end{bmatrix} = E_{\lambda} \begin{bmatrix} \hat{\boldsymbol{u}}_{\lambda}(\boldsymbol{r}) \\ \hat{\boldsymbol{v}}_{\lambda}(\boldsymbol{r}) \end{bmatrix}. \tag{10}$$

The eigen value E_{λ} is independent of spin channels because we consider unitary states in superconductors. In what follows, we briefly discuss the method to calculate the Josephson current for the d wave symmetry. The application to the p and the f wave symmetries is straightforward. In the case of the d wave symmetry, the BdG equation in eq. (10) is decoupled into two equations,

$$\sum_{\boldsymbol{r}'} \begin{bmatrix} h_{\boldsymbol{r},\boldsymbol{r}'} & d^{(d)}_{\boldsymbol{r},\boldsymbol{r}'} \\ \left(d^{(d)}_{\boldsymbol{r},\boldsymbol{r}'}\right)^{*} & -h^{*}_{\boldsymbol{r},\boldsymbol{r}'} \end{bmatrix} \begin{bmatrix} (u_{11})_{\lambda}(\boldsymbol{r}') \\ (v_{21})_{\lambda}(\boldsymbol{r}') \end{bmatrix} = E_{\lambda} \begin{bmatrix} (u_{11})_{\lambda}(\boldsymbol{r}) \\ (v_{21})_{\lambda}(\boldsymbol{r}) \end{bmatrix}, \tag{11}$$

where $\left(u_{ij}\right)$, for example, represents an element of $\hat{\boldsymbol{u}}$ in eq. (8) and $[u_{21}, v_{11}]^t$ obeys essentially the same equation. In the following, we omit 11 from u_{11} and 21 from v_{21}. The wave function can be represented in a $2M \times 1$ matrix form

$$\boldsymbol{\Psi}_{\lambda}(j) = \begin{pmatrix} u_{\lambda}(j\bar{\boldsymbol{x}} + 1\bar{\boldsymbol{y}}) \\ \vdots \\ u_{\lambda}(j\bar{\boldsymbol{x}} + M\bar{\boldsymbol{y}}) \\ v_{\lambda}(j\bar{\boldsymbol{x}} + 1\bar{\boldsymbol{y}}) \\ \vdots \\ v_{\lambda}(j\bar{\boldsymbol{x}} + M\bar{\boldsymbol{y}}) \end{pmatrix}. \tag{12}$$

For $j < -2$, for instance, the BdG equation reads

$$\begin{aligned} &\frac{\Delta}{2}\begin{pmatrix} \hat{0} & \mathrm{e}^{\mathrm{i}\varphi_{\mathrm{L}}}\hat{1} \\ \mathrm{e}^{-\mathrm{i}\varphi_{\mathrm{L}}}\hat{1} & \hat{0} \end{pmatrix}\boldsymbol{\Psi}_{\lambda}(j+2) \\ &\quad + \begin{pmatrix} \hat{T}_{\mathrm{N}}(-) & \hat{0} \\ \hat{0} & -\hat{T}_{\mathrm{N}}(-) \end{pmatrix}\boldsymbol{\Psi}_{\lambda}(j+1) \\ &\quad + \begin{pmatrix} -E_{\lambda}\hat{1} + \hat{E}_{\mathrm{S}} & \hat{0} \\ \hat{0} & -E_{\lambda}\hat{1} - \hat{E}_{\mathrm{S}} \end{pmatrix}\boldsymbol{\Psi}_{\lambda}(j) \\ &\quad + \begin{pmatrix} \hat{T}_{\mathrm{N}}(+) & \hat{0} \\ \hat{0} & -\hat{T}_{\mathrm{N}}(+) \end{pmatrix}\boldsymbol{\Psi}_{\lambda}(j-1) \\ &\quad + \frac{\Delta}{2}\begin{pmatrix} \hat{0} & \mathrm{e}^{\mathrm{i}\varphi_{\mathrm{L}}}\hat{1} \\ \mathrm{e}^{-\mathrm{i}\varphi_{\mathrm{L}}}\hat{1} & \hat{0} \end{pmatrix}\boldsymbol{\Psi}_{\lambda}(j-2) = 0, \end{aligned} \tag{13}$$

$$\hat{T}_{\mathrm{N}}(+) = \begin{pmatrix} -t_a & -t' & 0 & \cdots & 0 \\ 0 & -t_a & -t' & \cdots & 0 \\ \vdots & \ddots & \ddots & \ddots & \vdots \\ 0 & \cdots & 0 & -t_a & -t' \\ -t' & 0 & \cdots & 0 & -t_a \end{pmatrix}, \tag{14}$$

$$\hat{T}_{\mathrm{N}}(-) = \begin{pmatrix} -t_a & 0 & \cdots & 0 & -t' \\ -t' & -t_a & 0 & \cdots & 0 \\ \vdots & \ddots & \ddots & \ddots & \vdots \\ 0 & \cdots & -t' & -t_a & 0 \\ 0 & \cdots & 0 & -t' & -t_a \end{pmatrix}, \tag{15}$$

$$\hat{E}_{\mathrm{S}} = \begin{pmatrix} -\mu_{\mathrm{S}} & -t_b & 0 & \cdots & -t_b \\ -t_b & -\mu_{\mathrm{S}} & -t_b & \cdots & 0 \\ \vdots & \ddots & \ddots & \ddots & \vdots \\ 0 & \cdots & -t_b & -\mu_{\mathrm{S}} & -t_b \\ -t_b & 0 & \cdots & -t_b & -\mu_{\mathrm{S}} \end{pmatrix}, \tag{16}$$

where $\hat{1}$ and $\hat{0}$ are the $M \times M$ unit matrix and the zero matrix, respectively. To solve the BdG equation, we apply the recursive Green function method[49–51] and calculate the Matsubara Green function in a matrix form

$$\check{G}_{\omega_n}(j,j') = \sum_{\lambda} \boldsymbol{\Psi}_{\lambda}(j)[\mathrm{i}\omega_n - E_{\lambda}]^{-1}\boldsymbol{\Psi}^{\dagger}_{\lambda}(j'), \tag{17}$$

where $\omega_n = (2n+1)\pi T$ is the Matsubara frequency and T is a temperature. Throughout this paper, we use the units of $\hbar = k_{\mathrm{B}} = 1$, where k_{B} is the Boltzmann constant. The Josephson current in the insulator ($1 < j < L-1$) is given by[50,51]

$$J(j) = -\mathrm{i}eT\sum_{\omega_n} t_a \,\mathrm{Tr}\Big[\check{G}_{\omega_n}(j+1,j) - \check{G}_{\omega_n}(j,j+1)\Big]. \tag{18}$$

We note that $J(j)$ is independent of j when we consider the direct-current Josephson effect.

3. Josephson Current

The low-temperature anomaly of the Josephson current is a typical phenomenon in the quantum transport between two unconventional superconductors.[17–22,24,27] In this section, we discuss effects of the asymmetric second nearest neighbor hopping (t') on the ZES and on the Josephson current. For finite t', it is possible to consider two types of SIS junctions as shown in Figs. 1(a) and 1(b). The parallel junction consists of two A-type superconductors, whereas the mirror-type junction consists of a A-type superconductor and a B-type one. Generally speaking, the Josephson effects in the two junctions are not identical to each other.

In what follows, we choose the parameters as $t_b = 0.1t_a$, $\mu_{\mathrm{S}} = -1.4099t_a$, $\mu_{\mathrm{N}} = -2.0t_a$, $M = 20$, $L = 4$, and $V_{\mathrm{B}} = 2.0t_a$. The electron density is fixed at the quarter-filling. The amplitude of the pair potential at the zero temperature is $\Delta_0 = 0.1t_a$ and the dependence of the pair potential on temperatures is described by the BCS theory.

3.1 p Wave symmetry

In Fig. 2, we show the Josephson current in the parallel junction for the p wave symmetry. The vertical axis is

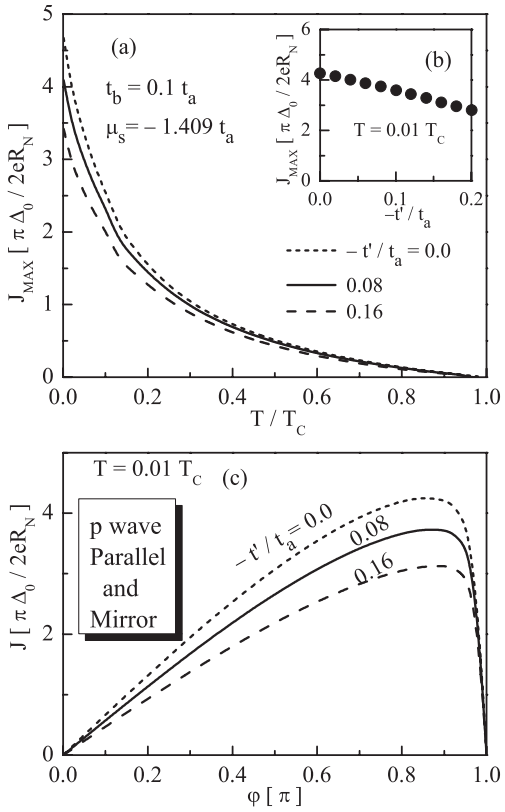

Fig. 2. Josephson current for the p wave symmetry is shown, where $t_b = 0.1t_a$, $\mu_S = -1.4099t_a$, $M = 20$, $L = 4$, and $V_B = 2t_a$. In (a), the maximum amplitude of the Josephson current (J_{max}) is plotted as a function of temperatures. In (b), J_{max} at $T = 0.01T_c$ are shown as a function of $-t'/t_a$. The current–phase relation is calculated at $T = 0.01T_c$ in (c).

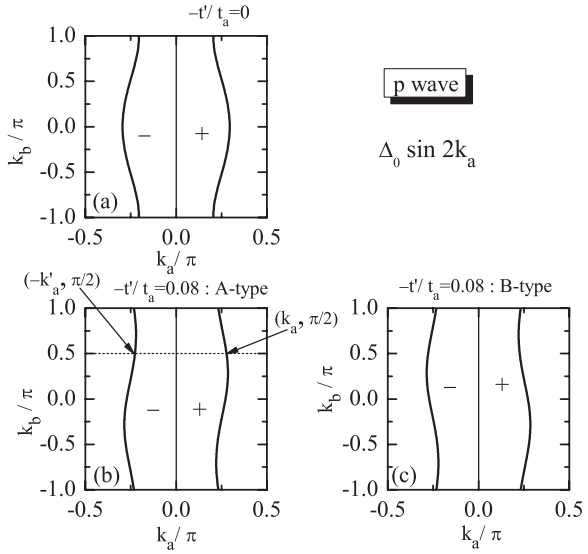

Fig. 3. The Fermi surface of TMTSF for $t' = 0$ is shown in (a). Those for $t' = -0.08t_a$ in the A-type and the B-type superconductors are shown in (b) and (c), respectively. The pair potential in the p wave symmetry is given by $\Delta \sin 2k_a$ which changes the sign at $k_a = 0$ as indicated by $+$ and $-$ in the figures.

normalized by $\pi\Delta_0/2eR_N$, where R_N is the normal resistance of junctions. We note in this vertical scale that the Josephson current of the s wave superconductor with the isotropic Fermi surface is close to unity in the limit of the zero temperature.[55] In $(TMTSF)_2PF_6$, the second nearest neighbor hopping is estimated as $-t'/t_a = 0.08$. We also show results for $-t'/t_a = 0$ and 0.16 for comparison. In Fig. 2(a), the maximum value of the Josephson current (J_{max}) is plotted as a function of temperatures, where J_{max} is obtained from the current–phase relation of the Josephson current. The Josephson current increases with decreasing temperatures for all t' and does not saturate even in low temperatures. This behavior is called the low-temperature anomaly of the Josephson current and is owing to the ZES at the junction interfaces. When the $\boldsymbol{d}$ vector has only one component, a condition for appearance of the ZES is given by[8]

$$\boldsymbol{d}(k_a, k_b) = -\boldsymbol{d}(-k_a, k_b), \tag{19}$$

where $\boldsymbol{d}(k_a, k_b)$ is the Fourier component of $\boldsymbol{d}_{r-r'}$. We note that eq. (19) is the most strict condition. The ZES can appear when $\boldsymbol{d}(k_a, k_b) \cdot \boldsymbol{d}(-k_a, k_b)$ is real negative.[8] The two pair potentials in eq. (19) correspond to the pair potentials in the electron and hole branches of a quasiparticle. Since the translational invariance in the y direction holds, k_b is conserved in the transmission and the reflection processes at the junction interfaces. In the p wave symmetry, a Fourier component of the pair potential in eq. (5) is given by

$$\boldsymbol{d}^{(p)}(k_a, k_b) = \Delta \sin(2k_a)\boldsymbol{e}_3. \tag{20}$$

Since eq. (20) is an odd function of k_a, it satisfies eq. (19) for all the Fermi surface as shown in Fig. 3, where we draw the Fermi surface for $t' = 0$ in (a), $t' = -0.08t_a$ in the A-type superconductor in (b) and $t' = -0.08t_a$ in the B-type superconductor in (c) with the solid line. The pair potential in the p wave symmetry has a node line at $k_a = 0$ in both the free electron model and the lattice model. In the lattice model, however, eq. (20) has *additional node lines* at $k_a = \pm 0.5\pi$ because of the pairing interaction between two electrons on the second nearest neighbor sites in the x direction as shown in Fig. 1. We define the *additional node lines* as the node lines resulting from the quarter-filling electron density.

The asymmetric hopping (t') modulates the shape of the Fermi surface as shown in Figs. 3(b) and 3(c). When the Fermi surface looses a symmetry with respect to $k_a = 0$, the condition for the ZES should be rewritten as

$$\boldsymbol{d}(k_a, k_b) \cdot \boldsymbol{d}(-k'_a, k_b) < 0, \tag{21}$$

where k_a and $-k'_a$ are the wave numbers on the Fermi surface. In Fig. 3(b), the two wave numbers are indicated by arrows on the Fermi surface for $k_b = \pi/2$. In the following, eq. (21) is referred to as the zero-energy condition (ZEC). Even in the presence of t', the ZEC is always satisfied because the additional node lines at $k_a = \pm\pi/2$ are far from the Fermi surface. The amplitude of the Josephson current at $T = 0.01T_c$ decreases with increasing $-t'/t_a$ as show in Fig. 2(b). This is mainly because R_N decreases with increasing $-t'/t_a$. In our calculation, R_N in units of h/e^2 are 1.04, 0.83 and 0.63 for $-t'/t_a = 0$, 0.08 and 0.16, respectively. In Fig. 2(c), we show the Josephson current as a function of $\varphi = \varphi_L - \varphi_R$ at $T = 0.01T_c$. The current–phase relation in the low temperature deviates from the sinusoidal function because the resonant tunneling through the ZES enhances the multiple Andreev reflection between the two

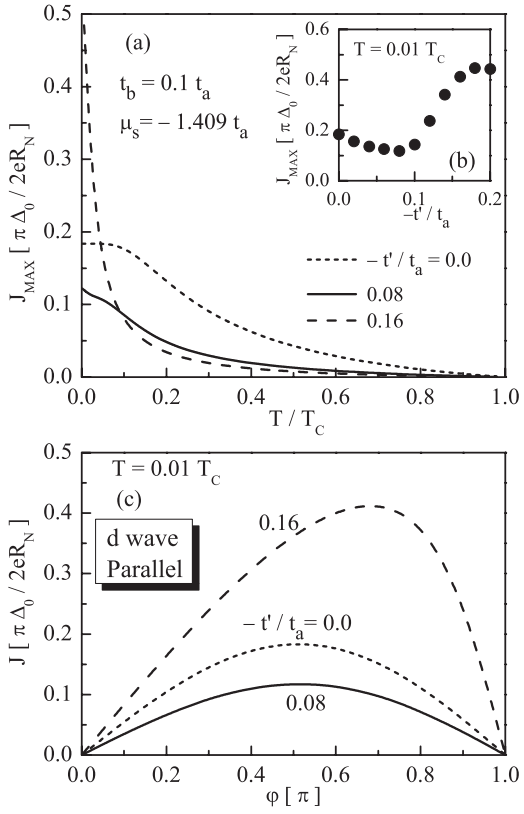

Fig. 4. Josephson current in the parallel junction for the d wave symmetry is shown. In (a), the Josephson current is plotted as a function of temperatures. In (b), amplitudes of the Josephson current at $T = 0.01T_c$ are shown as a function of $-t'/t_a$. The current–phase relation is calculated at $T = 0.01T_c$ in (c).

superconductors. We note that the results in the mirror-type junction are identical to those in Figs. 2(a)–2(c). In the p wave symmetry, the Josephson current is insensitive to the lattice structures because the ZES always forms at the junction interface irrespective of t'.

3.2 *d Wave symmetry*

In Fig. 4, we show the Josephson current in the parallel junctions for the d wave symmetry. In Fig. 4(a), J_{max} is plotted as a function of temperatures. In the absence of t', the Josephson current saturates in low temperatures as that in the s wave junctions. On the other hand, the results for $-t'/t_a = 0.08$ and 0.16 do not saturate in low temperatures. In particular, the Josephson current for $-t'/t_a = 0.16$ rapidly increases with decreasing temperatures. In the case of spin-singlet superconductors, the ZEC is given by

$$d(k_a, k_b)d(-k'_a, k_b) < 0, \tag{22}$$

where $d(k_a, k_b)$ is the Fourier component of $d_{\boldsymbol{r}-\boldsymbol{r}'}$. In the d wave symmetry, A Fourier component of the pair potential in eq. (6) is given by

$$d^{(d)}(k_a, k_b) = \Delta \cos(2k_a), \tag{23}$$

and is the even function of k_a. The additional node lines in the lattice model are at $k_a = \pm 0.25\pi$ and $\pm 0.75\pi$. In the absence of t', eq. (23) does not satisfy the ZEC in eq. (22) for all the Fermi surface as shown in Fig. 6, where we draw the Fermi surface for $t' = 0$ in (a). The Fermi surface indicated by the broken line does not satisfy the ZEC. In the presence of t', however, the ZEC can be satisfied for some wave numbers on the Fermi surface as plotted with the solid line in Fig. 6(b). The shape of the Fermi surface looses the inversion symmetry with respect to $k_a = 0$ in the presence of t'. As a result, the ZEC in eq. (22) is satisfied for some wave numbers on the Fermi surface because the Fermi surface lies along the additional node lines at $k_a = \pm 0.25\pi$. This implies an importance of lattice structures on the quantum transport. The current–phase relation deviates from the sinusoidal relation as shown in the results for $-t'/t_a = 0.16$ in Fig. 4(c) because most wave number on the Fermi surface satisfy the ZEC as shown in Fig. 6(d). We note that the Fermi surface around $k_b = 0$ and $\pm\pi$ are still out of the ZEC even for $-t'/t_a = 0.16$. In this paper, we consider relatively thick insulators, where the transmission probabilities of a quasiparticle incident perpendicular to the interface ($k_b \sim 0$) become much larger than those for $k_b \sim \pm\pi$. The contribution of the resonant tunneling via the ZES is small for $-t'/t_a = 0.08$ because the Fermi surface around $k_b \sim 0$ in Fig. 6(b) is out of the ZEC.

The Josephson effect in the mirror-type junctions is qualitatively different from that in the parallel junctions. In Fig. 5, we show the Josephson current for the d wave symmetry in the mirror-type junctions. In Fig. 5(a), J_{max} for $-t'/t_a = 0.08$ first increases with decreasing temperatures then decreases for $T < 0.05T_c$. Such a non monotonic temperature dependence has been also reported in the high-T_c superconductor Josephson junctions. For $-t'/t_a = 0.16$, the Josephson current changes its sign and the amplitude increases rapidly with decreasing temperatures. The dif-

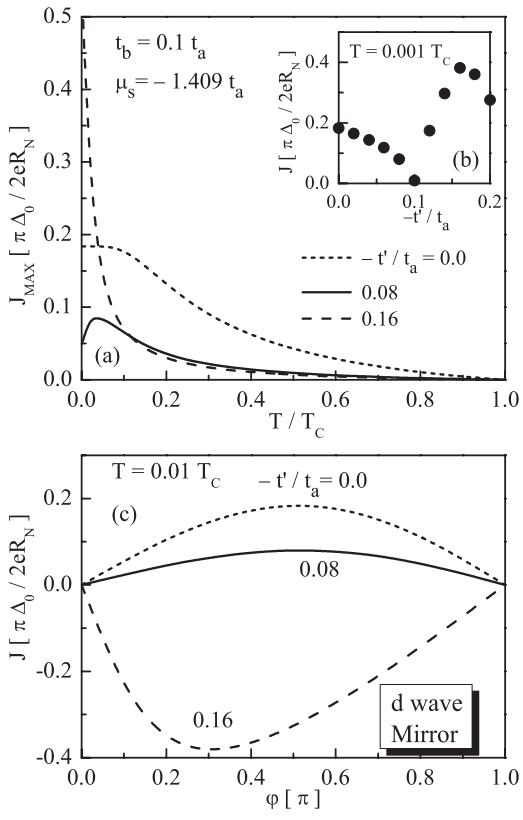

Fig. 5. Josephson current for the d wave symmetry in the mirror-type junction.

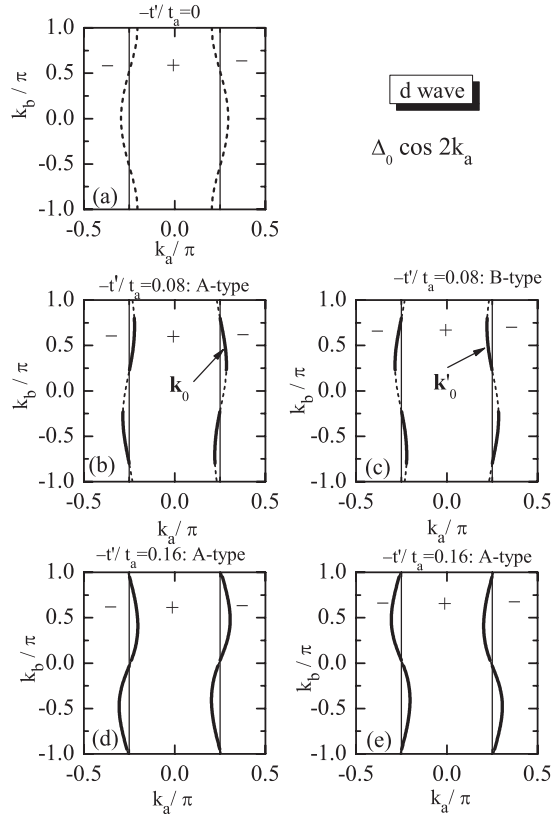

Fig. 6. The Fermi surface of TMTSF for $t' = 0$ is shown in (a). Those for $t' = -0.08t_a$ in the A-type and the B-type superconductors are shown in (b) and (c), respectively. The pair potential in the d wave symmetry is given by $\Delta \cos 2k_a$ which changes its sign at $k_a = \pm 0.25\pi$ as indicated by $+$ and $-$ in the figures. The Fermi surface for $t' = -0.16t_a$ is shown for A-type and B-type superconductors in (d) and (e), respectively. The Fermi surface shown with the solid line satisfy the condition for the ZES in eq. (22).

ferences between the parallel and the mirror-type junctions can be understood in terms of the relative sign of the pair potentials in the two superconductors. In the presence of the time-reversal symmetry, the Josephson current is decomposed into a series of

$$J = \sum_{n=1}^{\infty} J_n \sin(n\varphi). \tag{24}$$

It was shown that the J_1 is roughly given by[22)]

$$J_1 = \sum_{k_b} d_{\mathrm{R}}(k'_a, k_b) d_{\mathrm{L}}(k_a, k_b) F_1(k_b), \tag{25}$$

where F_1 is the positive function of k_b, $d_{\mathrm{R}}(k'_a, k_b)$ and $d_{\mathrm{L}}(k_a, k_b)$ are the pair potential on the Fermi surface in the right and the left superconductors, respectively. Thus the product of $d_{\mathrm{R}}(k'_a, k_b) d_{\mathrm{L}}(k_a, k_b)$ determines the sign of the Josephson current which is proportional to $\sin\varphi$. The parallel junction consists of two A-type superconductors as shown in Fig. 1. Therefore $d_{\mathrm{R}}(k_a, k_b)$ and $d_{\mathrm{L}}(k_a, k_b)$ are identical to each other, which results in the positive sign of J_1. On the other hand in the mirror-type junctions, $d_{\mathrm{L}}(\boldsymbol{k}_0)$ in the A-type superconductor shown in Fig. 6(b) has the opposite sign to $d_{\mathrm{R}}(\boldsymbol{k}'_0)$ in the B-type superconductor in (c). In the mirror-type junctions, it is easily shown that $d_{\mathrm{R}}(k'_a, k_b) d_{\mathrm{L}}(k_a, k_b)$ is always negative (positive) for a quasiparticle satisfying (not satisfying) the ZEC. In high temperatures, J_1 becomes positive because a quasiparticle for $k_b \sim 0$ (which is out of the ZEC) mainly contributes to the Josephson current. In low temperatures, the resonant transmission via the ZES also contributes to the Josephson current. As a consequence, J_1 has a non monotonic temperature dependence as shown in Fig. 5(a). For $-t'/t_a = 0.16$, the Josephson current is negative for low temperatures because the resonant transmission via the ZES mainly contributes to the Josephson current. It is also shown that the Josephson current proportional to $\sin 2\varphi$ is given by

$$J_2 = -\sum_{k_b} \left[d_{\mathrm{R}}(k_a, k_b) d_{\mathrm{L}}(k'_a, k_b) \right]^2 F_2(k_b), \tag{26}$$

where F_2 is the positive function of k_b. The sign of J_2 is always negative irrespective of the pairing symmetries of the two superconductors. Thus the current–phase relation for $-t'/t_a = 0.16$ in Fig. 4(c) shows the maximum at $\varphi > 0.5\pi$ in the parallel junctions. While the current–phase relation in the mirror-type junction takes its minimum at $\varphi < 0.5\pi$ as shown in Fig. 5(c).

3.3 f Wave symmetry

In Fig. 7, we show the Josephson current for the f wave symmetry in the parallel junctions. In Fig. 7(a), the maximum amplitude of the Josephson current is plotted as a function of temperatures for $-t'/t_a = 0, 0.08$ and 0.16. In the absence of t', the Josephson current show the low-temperature anomaly because the Fourier component of the

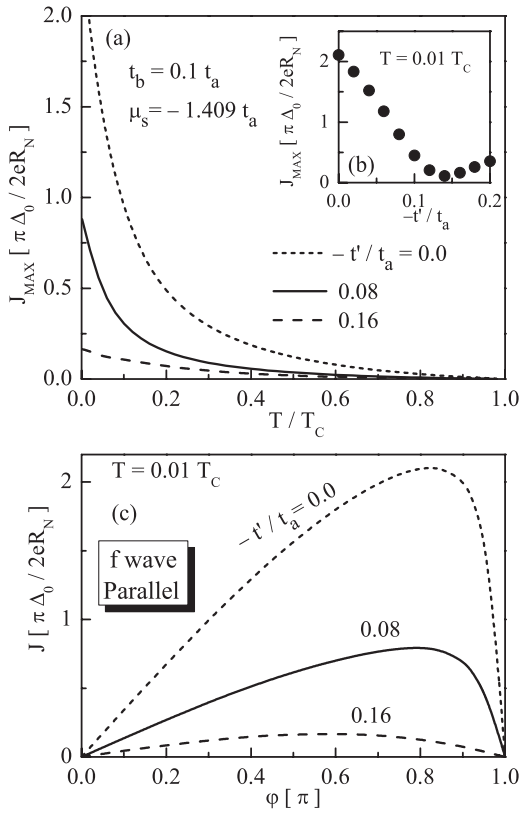

Fig. 7. Josephson current for f wave symmetry in the parallel junctions. In (a), the maximum amplitude of the Josephson current is plotted as a function of temperatures. In (b), amplitudes of the Josephson current at $T = 0.01T_{\mathrm{c}}$ are shown as a function of $-t'/t_a$. The current–phase relation is calculated at $T = 0.01T_{\mathrm{c}}$ in (c).

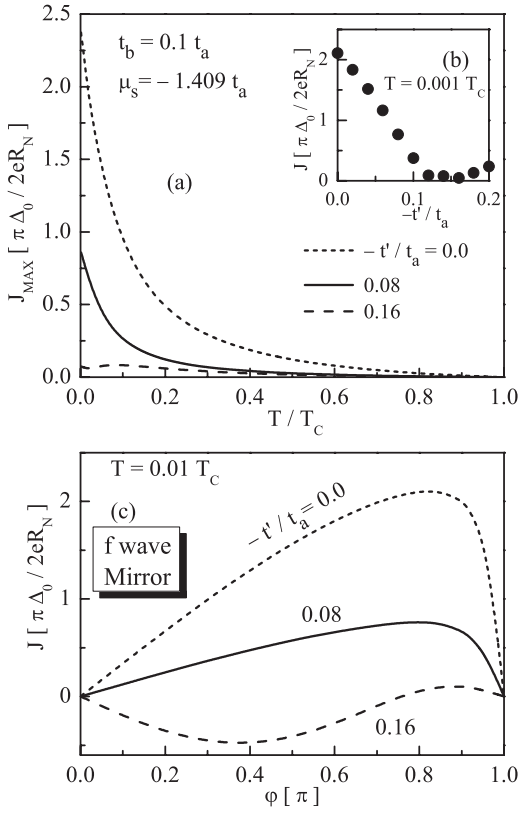

Fig. 8. Josephson current for f wave symmetry in the mirror-type junctions.

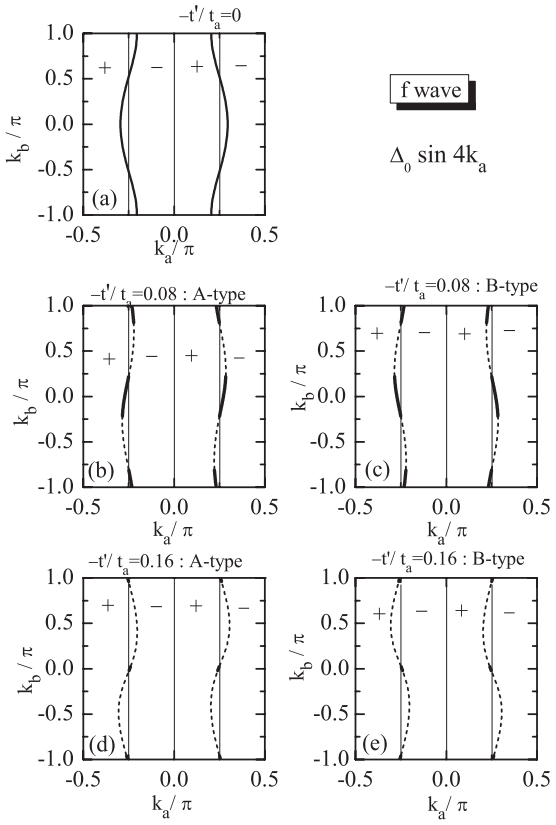

Fig. 9. The Fermi surface of TMTSF for $t' = 0$ is shown in (a). Those for $t' = -0.08t_a$ in the A-type and the B-type junctions are shown in (b) and (c), respectively. The Fermi surface for $t' = -0.16t_a$ is shown in (d) and (e). The pair potential in the f wave symmetry is given by $\Delta \sin 4k_a$ which changes the sign at $k_a = 0$ and $\pm 0.25\pi$ as indicated by $+$ and $-$ in the figures. The Fermi surface shown with the solid line satisfies the condition for the ZES. The broken line indicates the wave numbers of the Fermi surface which do not satisfy the condition of the ZES.

pair potential, $\Delta \sin 4k_a$, satisfies the ZEC for all the Fermi surface as shown in Fig. 9(a). The additional node lines are at $k_a = \pm 0.25\pi$, $\pm 0.5\pi$ and $\pm 0.75\pi$ in the lattice model. The anomalous behavior tends to disappear for finite t'. In Fig. 9(b), the Fermi surface out of the ZEC is indicated by the broken line for $t' = -0.08t_a$. For $t' = -0.16t_a$, most wave numbers of the Fermi surface do not satisfy the ZEC as shown in Fig. 9(d). In contrast to the d wave junctions, the formation of the ZES is suppressed by introducing t' in the f wave junctions. The phase–current relation for $-t'/t_a = 0$ and 0.08 in Fig. 7(c) apparently deviates from the sinusoidal function because of the multiple Andreev reflection via the ZES. The results for $-t'/t_a = 0.16$ slightly deviate from $\sin\varphi$, but degree of deviation is smaller than those for $-t'/t_a = 0$ and 0.08.

In Fig. 8, we show the Josephson current for the f wave symmetry in the mirror-type junctions. In (a), the Josephson current for $-t'/t_a = 0$ and 0.08 are essentially the same as those in the parallel junctions. In the current–phase relation for $-t'/t_a = 0.16$ in (c), the Josephson current becomes zero around $\varphi = 0.75\pi$. In this case, J_1 becomes negative because $\boldsymbol{d}_{\rm R}(k'_a, k_b) \cdot \boldsymbol{d}_{\rm L}(k_a, k_b)$ is negative for almost all the Fermi surface. The amplitude of J_2 is not negligible because of the resonant transmission through the ZES for a quasiparticle incident perpendicular to the interface (i.e., $k_b \sim 0$). In a rough estimation, we find $|J_2| \sim 0.7|J_1|$.

4. Discussion

So far, we have studied the tunneling spectra and the Josephson current of unconventional superconductors in both the free electron model and the lattice model. In the case of high-T_c superconductors, we find no qualitative differences between the calculated results in the two theoretical models. Indeed, the theoretical results in the free electron model well explain the experimental results. Thus the formation of the ZES has been believed to be insensitive to electronic structures in superconductors such as the effective mass of an electron and the shape of the Fermi surface. The calculated results in this paper, however, indicate that this statement is justified when the Fermi surface is far from the *additional node lines* peculiar to the lattice model. At the quarter-filling electron density of Q1D superconductors, the pairing interaction tends to work between two electrons at the second nearest neighbor sites in the x direction as shown in Fig. 1 because of the long range Coulomb repulsion. In particular, the f wave superconductivity requires the pairing interaction between the fourth nearest neighbor sites in the x direction. As a consequence, the pair potential changes its sign at the additional node lines at $k_a = \pm 0.25\pi$ in the d and f wave symmetries as shown in Figs. 6 and 9. In the absence of the asymmetric hopping (t'), it is clear that the ZES is (not) formed in the f (d) wave symmetry. This is because the pair potential in the f wave (d wave) symmetry is an odd (even) function of k_a. In the presence of t', the shape of the Fermi surface looses the inversion symmetry with respect to k_a, which affects the formation of the ZES. Roughly speaking, t'

assists the formation of the ZES in the d wave symmetry, whereas it suppresses the ZES in the f wave symmetry. As a results, the Josephson current exhibit the various temperature dependences and the phase–current relations depending on the pairing symmetries, the degree of asymmetry and the types of junctions.

The formation of the ZES is a universal phenomenon at the surface of unconventional superconductors.[8] It may be possible to analyze the pairing symmetry of unconventional superconductors from the anisotropy in the tunneling conductance and that in the Josephson current because these transport properties reflect the internal information of Cooper pairs. In particular, tunneling spectroscopy is a useful tool to analyze the pairing symmetry.[29,32] In experiments, however, the tunneling measurement has never been done because it may be difficult to have clean and stable surfaces of such organic materials. We are thinking that it may be slightly easier to fabricate Josephson junctions from bulk superconductors. It would be possible to introduce a weak link on a bulk superconductor by using, for example, the ion-beam irradiation technique or electro-crystallization technique on bicrystals.[37] The calculated results, by the first looking, imply that it may be impossible to specify the pairing symmetry of the organic superconductors because the low-temperature anomaly can be observed for all candidates of pairing symmetries. In the previous paper, however, we showed that the sensitivity of the ZES to external magnetic fields depends strongly on the pairing symmetries.[29] Thus it would be possible to extract information of the pairing symmetry from the characteristic behavior of the Josephson current under magnetic fields. The results of this paper is the first step to discuss this issue. In our model, the external magnetic fields can be taken into account through the Peierls phase of the hopping integral. The investigation in this direction is in progress. Results will be given elsewhere soon.

5. Conclusion

We have studied the Josephson current in quasi one-dimensional unconventional superconductors at the quarter-filling electron density by using the tight-binding model on a two-dimensional square lattice. The triangular lattice structure is also considered by the asymmetric second nearest neighbor hopping (t') introduced on the square lattice. The theoretical model describes electronic structures of organic superconductors such as $(TMTSF)_2X$. In the calculation, we assume p, d, and f wave like pairing symmetries in superconductors. The pair potentials have the *additional node lines* because the pairing interaction works between the second or fourth nearest neighbor sites in the current direction at the quarter-filled electron density. The formation of the zero-energy states is sensitive to t' in the d and f wave symmetries because the Fermi surface lies just along the additional node lines at $k_a = \pm 0.25\pi$. In the presence of t', the triangular lattice structure assists the formation of the ZES in the d wave symmetry, whereas it suppresses the ZES in the f wave symmetry. It is possible to consider the two types of junctions, (i.e., parallel and mirror), because of the triangular lattice structures. The Josephson current shows various temperature dependences and current–phase relations depending on the pairing symmetries of superconductors, the shape of the Fermi surface and the types of the junction.

1) A. F. Andreev: Zh. Eksp. Teor. Fiz. **46** (1964) 1823 [Sov. Phys. JETP **19** (1964) 1228].
2) A. Furusaki and M. Tsukada: Solid State Commun. **78** (1991) 299.
3) L. J. Buchholtz and G. Zwicknagl: Phys. Rev. B **23** (1981) 5788.
4) C. R. Hu: Phys. Rev. Lett. **72** (1994) 1526.
5) Y. Tanaka and S. Kashiwaya: Phys. Rev. Lett. **74** (1995) 3451.
6) S. Kashiwaya and Y. Tanaka: Rep. Prog. Phys. **63** (2000) 1641.
7) T. Löfwander, V. S. Shumeiko and G. Wendin: Supercond. Sci. Technol. **14** (2001) R53.
8) Y. Asano, Y. Tanaka and S. Kashiwaya: Phys. Rev. B **69** (2004) 134501.
9) Y. Asano, Y. Tanaka and S. Kashiwaya: Phys. Rev. B **69** (2004) 214509.
10) S. Kashiwaya, Y. Tanaka, M. Koyanagi, H. Takashima and K. Kajimura: Phys. Rev. B **51** (1995) 1350.
11) J. Y. T. Wei, N.-C. Yeh, D. F. Garrigus and M. Strasik: Phys. Rev. Lett. **81** (1998) 2542.
12) I. Iguchi, W. Wang, M. Yamazaki, Y. Tanaka and S. Kashiwaya: Phys. Rev. B **62** (2000) R6131.
13) Z. Q. Mao, M. M. Rosario, K. D. Nelson, K. Wu, I. G. Deac, P. Schiffer, Y. Liu, T. He, K. A. Regan and R. J. Cava: Phys. Rev. B **67** (2003) 094502.
14) M. Yamashiro, Y. Tanaka and S. Kashiwaya: Phys. Rev. B **56** (1997) 7847.
15) Y. Asano, Y. Tanaka, Y. Matsuda and S. Kashiwaya: Phys. Rev. B **68** (2003) 184506.
16) Y. Tanaka, Yu. V. Nazarov and S. Kashiwaya: Phys. Rev. Lett. **90** (2003) 167003.
17) Y. S. Barash, H. Burkhardt and D. Rainer: Phys. Rev. Lett. **77** (1996) 4070.
18) Y. Tanaka and S. Kashiwaya: Phys. Rev. B **53** (1996) 9371.
19) Y. Tanaka and S. Kashiwaya: Phys. Rev. B **53** (1996) R11957.
20) Y. Tanaka and S. Kashiwaya: Phys. Rev. B **56** (1997) 892.
21) Y. Tanaka and S. Kashiwaya: Phys. Rev. B **58** (1998) R2948.
22) Y. Asano: Phys. Rev. B **64** (2001) 224515.
23) Yu. S. Barash, A. M. Bobkov and M. Fogelstrom: Phys. Rev. B **64** (2001) 214503.
24) Y. Asano and K. Katabuchi: J. Phys. Soc. Jpn. **71** (2002) 1974.
25) Y. Asano, Y. Tanaka, M. Sigrist and S. Kashiwaya: Phys. Rev. B **67** (2003) 184505.
26) S. Shirai, H. Tsuchiura, Y. Asano, Y. Tanaka, J. Inoue, Y. Tanuma and S. Kashiwaya: J. Phys. Soc. Jpn. **72** (2003) 2299.
27) Y. Asano: Phys. Rev. B **64** (2001) 014511.
28) Y. Asano: J. Phys. Soc. Jpn. **71** (2002) 905.
29) Y. Tanuma, K. Kuroki Y. Tanaka, R. Arita, S. Kashiwaya and H. Aoki: Phys. Rev. B **66** (2002) 094507.
30) D. Jerome, A. Mazaud, M. Ribault and K. Bechgaad: J. Phys. Lett. (Paris) **41** (1980) L92.
31) K. Bechgaad, K. Carneiro, M. Olsen, F. B. Rasmussen and C. S. Jacobsen: Phys. Rev. Lett. **46** (1981) 852.
32) Y. Tanuma, Y. Tanaka, K. Kuroki and S. Kashiwaya: Phys. Rev. B **64** (2001) 214510.
33) I. J. Lee, M. J. Naughton, G. M. Danner and P. M. Chaikin: Phys. Rev. Lett. **78** (1997) 3555; I. J. Lee, P. M. Chaikin and M. J. Naughton: Phys. Rev. B **62** (2000) R14669.
34) I. J. Lee, S. E. Brown, W. G. Clark, M. J. Strouse, M. J. Naughton, W. Kang and P. M. Chaikin: Phys. Rev. Lett. **88** (2002) 017004.
35) M. Takigawa, H. Yasuoka and G. Saito: J. Phys. Soc. Jpn. **56** (1987) 873.
36) S. Belin and K. Behnia: Phys. Rev. Lett. **79** (1997) 2125.
37) H. I. Ha, J. I. Oh, J. Moser and M. J. Naughton: Synth. Met. **137** (2003) 1215.
38) A. A. Abrikosov: J. Low. Temp. Phys. **53** (1983) 359.
39) Y. Hasegawa and H. Fukuyama: J. Phys. Soc. Jpn. **56** (1987) 877.
40) A. G. Lebed: Phys. Rev. B **59** (1999) R721; A. G. Lebed, K. Machida and M. Ozaki: *ibid.* **62** (2000) R795.
41) H. Shimahara: J. Phys. Soc. Jpn. **58** (1989) 1735.
42) K. Kuroki and H. Aoki: Phys. Rev. B **60** (1999) 3060.
43) H. Kino and H. Kontani: J. Low Temp. Phys. **117** (1999) 317.

44) K. Kuroki, R. Arita and H. Aoki: Phys. Rev. B **63** (2001) 094509.
45) J. P. Pouget and S. Ravy: J. Phys. I (Paris) **6** (1996) 1501.
46) S. Kagoshima, Y. Saso, M. Maesato, R. Kondo and T. Hasegawa: Solid State Commun. **110** (1999) 479.
47) C. D. Vaccarella, R. D. Duncan and C. A. R. Sa de Melo: Physica C **391** (2003) 89.
48) H.-J. Kwon, K. Senguputa and V. M. Yakovenko: cond-mat/0210148.
49) P. A. Lee and D. S. Fisher: Phys. Rev. Lett. **47** (1981) 882.
50) A. Furusaki: Physica B **203** (1994) 214.
51) Y. Asano: Phys. Rev. B **63** (2001) 052512.
52) K. Mortensen, Y. Tomkiewicz, T. D. Schults and E. M. Engler: Phys. Rev. Lett. **46** (1981) 1234.
53) M. Matsumoto and H. Shiba: J. Phys. Soc. Jpn. **64** (1995) 3384; *ibid.* **64** (1995) 4867.
54) P. G. de Gennes: *Superconductivity of Metals and Alloys* (Benjamin, New York, 1966).
55) V. Ambegaokar and A. Baratoff: Phys. Rev. Lett. **10** (1963) 486.